

Communication

# Rapid Degradation of Azo Dyes by Melt-Spun Mg-Zn-Ca Metallic Glass in Artificial Seawater

Peng Chen, Ximei Hu, Yumin Qi, Xin Wang \*, Zongjia Li, Lichen Zhao, Shuiqing Liu and Chunxiang Cui \*

Key Laboratory for New Type of Functional Materials in Hebei Province, School of Material Science and Engineering, Hebei University of Technology, Tianjin 300130, China; m15900225021@163.com (P.C.); huximei@hebut.edu.cn (X.H.); qiyuminabc@163.com (Y.Q.); zongjial@126.com (Z.L.); zhlch@hebut.edu.cn (L.Z.); liushuiqing0824@126.com (S.L.)

\* Correspondence: ahaxin@hebut.edu.cn (X.W.); hutcui@hebut.edu.cn (C.C.); Tel.: +86-022-6020-2194 (X.W.); +86-022-2656-4125 (C.C.); Fax: +86-022-6020-4125 (X.W. & C.C.)

Received: 17 October 2017; Accepted: 5 November 2017; Published: 8 November 2017

**Abstract:** Mg-Zn-Ca metallic glass (MG) is effective for degrading azo dyes; however, the related surface evolution and degradation mechanisms are little known. We comparatively investigated the initial surface corrosion morphologies of melt-spun  $Mg_{66}Zn_{30}Ca_4$  MG in deionized water and artificial seawater. It was found that the basic corrosion behavior of the MG was the same, except that the corrosion process was accelerated in seawater. The presence of NaCl obviously promotes the formation of nano-ZnO on the surface of ribbons, causing the rapid degradation of azo dyes due to the photocatalytic effect. The degradation efficiency when combined with 3.5 wt % NaCl was over 100 times higher than that without NaCl. This indicates that Mg-Zn-Ca MG ribbons are effective additives for the degradation of azo dyes in seawater.

**Keywords:** metallic glass; Mg-Zn-Ca; corrosion; azo dyes degradation

## 1. Introduction

The degradation of azo dyes is one of the most important aspects in sewage treatments, and has attracted extensive attention in the field of environment protection engineering. In 2012, Wang et al. demonstrated that Mg-Zn-Ca metallic glass (MZC MG) can effectively degrade azo dyes, and that the degradation ability of amorphous alloys is much better than that of their crystalline counterparts [1]. As an agent or catalyst for sewage treatment, MZC glassy alloy can be discharged directly into the environment without needing to be recovered, due to the degradability of MZC MG itself. In addition, Mg-Zn-Ca alloys are environmentally friendly alloys, because the main elements of the alloys are non-toxic and safe, and will not cause secondary pollution when the elements are dissolved in the natural water system. The degradation process of azo dyes driven by MZC MG is a complex chemical process that is constrained by many factors, such as pH value of the solution, chemical composition of MZC alloy, size of powder, and residual stress [1–3]. However, the reaction occurring on the surface of MZC MG and the degradation mechanism between MZC amorphous alloys and azo dyes still remain unclear.

The fabrication methods and different additional treatments can obviously affect the degradation ability of metallic glasses (MGs). Different fabrications usually induce different statuses of MG products, which may strongly affect the efficiency of the MG. Powders, glassy thin films [4] or melt-spun ribbons [5–7] are also used in water treatments. Melt spinning is a widely used technology in typical industrial fields [8,9], and thus the ribbons are easy to fabricate. By minor alloying of the ribbon, the mechanical properties and functional properties of the ribbon can be changed and improved [10]. For example, different alloying elements can obviously influence the degradation mechanism and the

degradation efficiency of Fe-Si-B alloys [11]. Since ribbon samples are beneficial to the experimental operation, the degradation mechanism of MG were also investigated based on the ribbons. Most related reports have demonstrated that the degradation efficiency is greatly deteriorated after annealing treatment due to the disappearance of residual stress and metastable structure [1,5,6,12]. However, several recent reports have shown that the chemical heterogeneity of nanocrystals caused by annealing may be beneficial for the degradation of azo dyes. Xie et al. [13] reported that Fe heterogeneity improves the degradation capability of  $\text{Fe}_{76}\text{B}_{12}\text{Si}_9\text{Y}_3$  amorphous powders, which has been attributed to the accelerated corrosion of the Fe-rich region, which tends to lose electrons. Similarly, the nanocrystals in Fe-based amorphous composite alloys can also induce the fast corrosion of  $\alpha$ -Fe, and were found to significantly improve degradation efficiency [7,14]. That is to say, the accelerated corrosion of MG is beneficial to the fast degradation of azo dyes, and therefore needs further investigation with respect to other MG alloys.

In order to verify the viewpoint that the accelerated corrosion is related to the degradation mechanism, we carefully compared the initial corrosion behavior of MZC MG in deionized water (DW) and in artificial seawater (ASW, 3.5 wt % NaCl, used for an accelerated corrosion condition). The efficiency of MZC ribbon in degrading azo dyes will also be examined in artificial waste water prepared with both DW and ASW.

## 2. Materials and Methods

High-purity (99.99 wt %) Mg, Zn and Ca elements were used as raw materials to prepare the master alloy  $\text{Mg}_{66}\text{Zn}_{30}\text{Ca}_4$  [15]. The master alloy ingots were re-melted by induction melting and sprayed onto a copper roller at a rotating rate of 2000 r/min to obtain the ribbons (the schematic diagram of the equipment is described in detail elsewhere [16]). This technique is the so-called melt spinning, which has become a novel method for fabricating MG ribbons. The as-spun ribbons were cut into small pieces with a size of ~2 mm for degrading azo dyes. Two azo dye solutions were prepared by the Direct Blue 6 (DB6,  $\text{C}_{32}\text{H}_{20}\text{N}_6\text{Na}_4\text{O}_{14}\text{S}_4$ ), which was dissolved in DW and ASW, in turn, with a concentration of 0.2 g/L. For each test, 0.3 g of MZC powder was added into 100 mL azo dye solutions under magnetic stirring. After stirring for specified times, ~2 mL solution was taken out and filtered to measure the absorbance by ultraviolet-visible (UV) spectrophotometry at a wavelength of 580 nm. The amorphous structure of the ribbon samples was confirmed by X-ray diffractometry (XRD, Bruker D8 Advance, Cu K $\alpha$ ; Bruker, Billerica, MA, USA). The corrosion morphology was studied by scanning electron microscope (SEM, Hitachi S-4800; Hitachi, Tokyo, Japan). The pH change of the treated solutions was determined by pH meter (PHS-3CB; Shanghai Yueping Scientific Instrument Co., Ltd., Shanghai, China). Open circuit potential (OCP) tests of the ribbons were performed on an electrochemical measurement system (LK3200A; Lanlike Chemical Electronic High-Tech Co., Ltd., Tianjin, China), using a saturated calomel electrode as reference electrode.

## 3. Results

Figure 1 shows the morphology evolution on the surface of MZC MG ribbon in DW and ASW solution. For the DW sample, as shown in Figure 1a–c, the basic process on the surface of the MZC sample results in the growth of whisker-like reaction products. With an immersion time of 30 min, some small whisker-like particles begin to appear and form a discontinuous network on the surface. When the time reaches 60 min, the whisker-like particles grow and form a continuous network. Up until 120 min later, the networks become more and more intensive. For the ASW sample, as shown in Figure 1d–f, the basic corrosion behavior is similar to DW, except that the detailed process is obviously accelerated. As a result, the density of the whiskers on the ASW sample with an immersion time of 5 min, as shown in Figure 1d, is comparable to that of DW sample with an immersion time of 1 h, as shown in Figure 1b. In addition, for the ASW sample at 30 min, as shown in Figure 1e, there are a lot of small plates with a size of ~500 nm lying on the surface of the sample that seem to be peeling off from the network and being adsorbed on the surface. It is demonstrated that the white whisker-like

products shown in Figure 1a–d are actually plates with a thickness of ~20 nm, standing upright on the surface.

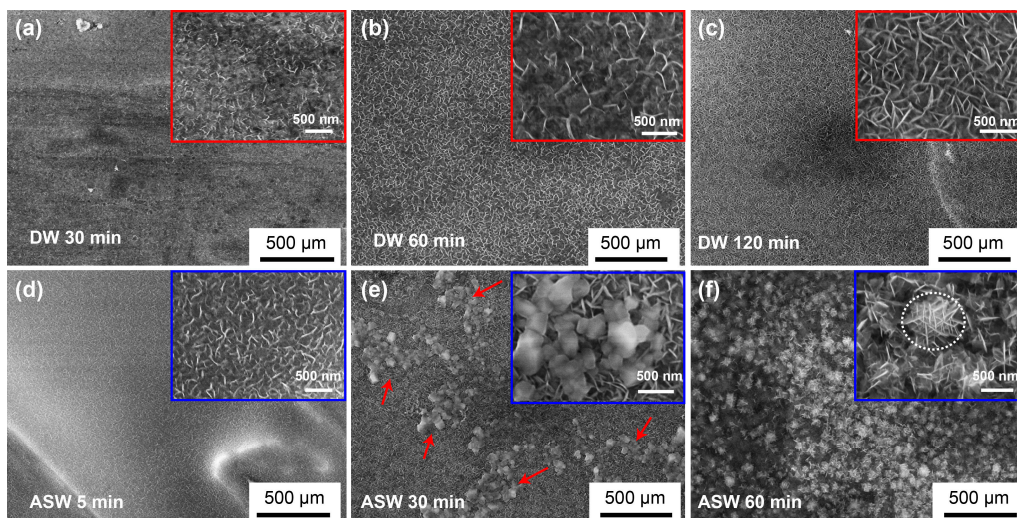


**Figure 1.** The surface morphology of MZC MG (Mg-Zn-Ca metallic glass) ribbon after being treated for different times in DW (deionized water) solution (a–c) and ASW (artificial seawater) solution (d–f), with an inset in each picture showing its respective high-magnification image.

Figure 2 shows the XRD spectra of the MZC ribbons after 2 h of immersion in different sewage. For the ribbon samples treated in DW, the XRD spectrum before and after the immersion is basically the same, showing a typical amorphous structure. It indicates that the nano-plates on the surface of the MZC ribbons may be some amorphous products, or the amount of crystalline nano-plate is too small to be detected by the used X-ray diffractometer. However, for the spectrum of the ASW sample, two diffraction peaks of Zn appear, indicating that the nano-plate networks in Figure 1 may be the residual Zn after removal of Mg and Ca from the surface of MZC MG ribbons.

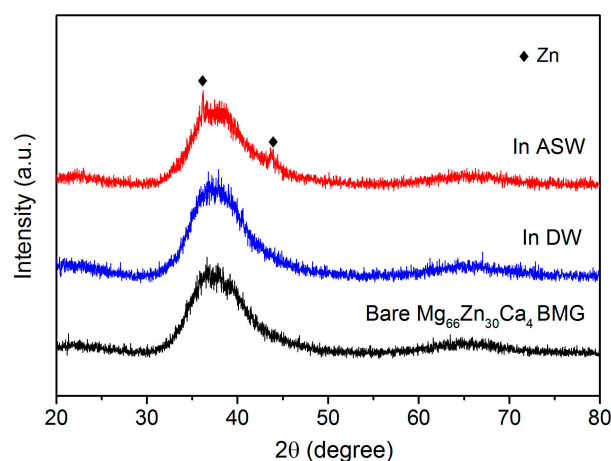


**Figure 2.** XRD (X-ray diffractometry) spectra of MZC ribbons after different treatments (BMG: Bulk metallic glass).

Figure 3 shows the degradation results of MZC ribbon samples comparatively in two sewage solutions. For the DW solution, the azo dye is completely degraded after approximately 2 h, which is much slower than the time required for balling powders and atomized powders [1,2]. The degradation efficiency of MZC alloy generally depends on the size of the powders, which determines the specific

surface area. The size of the ribbons used in this work is much larger than that of balling powders and atomized powders, so the actual contact area, as well as the degrading reaction area between MZC MG and DB6, is relatively small. With the same size of ribbon fragments, MZC ribbon shows a greater ability to degrade azo dye in the ASW solution. In particular, after being immersed for only 60 s, the degradation of azo dyes is almost complete, which is over 100 times faster than with DW. In other words, seawater is an ideal environment for MZC MG ribbons to degrade azo dyes.

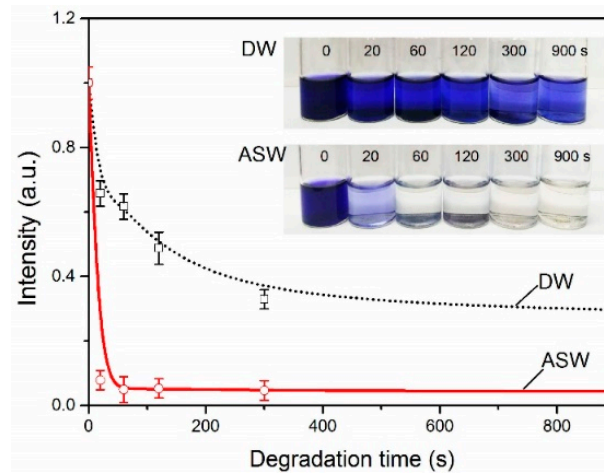


**Figure 3.** The normalized absorbency as a function of treatment time in the DW and ASW solution, with the inset showing the color change of the treated solutions.

Figure 4a shows the OCP test curves for MZC samples treated in DW and ASW sewage solutions, respectively. It is obvious that the electrode potential of MZC in ASW is much lower than that in DW. This indicates that the tendency of MZC MG to lose electrons in ASW is greater than that in DW, leading to a higher corrosion rate. It is worth noting that the time required for the OCP to increase from the beginning to a near-steady value is ~50 s in the ASW (marked by an arrow on the curves), which is much shorter than that required in the DW (200 s). Similarly, the change in pH of the soaking solution exhibits a similar phenomenon. Figure 4b shows the curves of pH vs. treatment time in DW and ASW sewage solutions that have been treated using MZC ribbons, with the same amount added. The rate of pH increase for ASW is much higher than that for DW when the immersion time is less than 10 h.

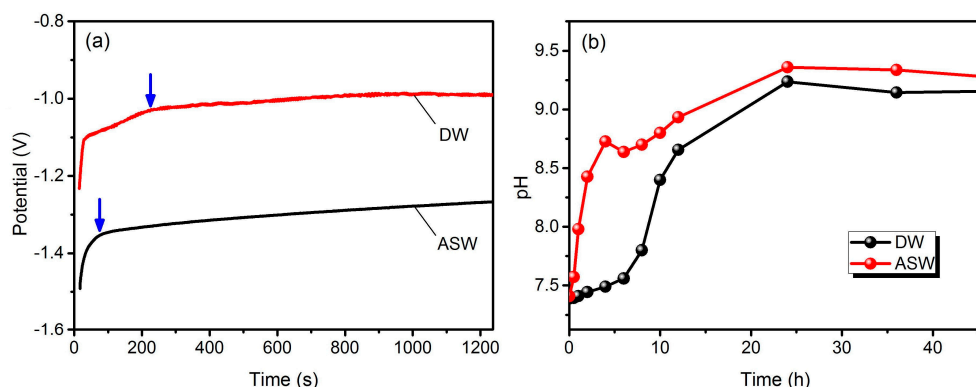


**Figure 4.** (a) The OCP (Open circuit potential) curves of MZC ribbon in ASW and DW solutions and (b) The pH value of the treated ASW and DW solution immersed in MZC ribbons for various times.

#### 4. Discussion

In essence, the mechanism of MZC MG in degrading azo dyes is related to its corrosion behavior in sewage solutions. For Mg-Zn-Ca system, the glass-forming ability (GFA) of the alloys is not so good [17,18]. Ribbon samples can be relatively easily prepared with full-amorphous structures due to their fast cooling rate during melt-spinning, and the mechanical properties are generally good, when compared with the bulk samples, because of the size effect [19,20]. Moreover, ribbon samples are easier to treat than powder samples or during corrosion experiments. Therefore we use ribbons as the experimental materials to investigate the corrosion behavior and surface morphology evolution of MZC, as shown in Figure 1. In fact, the basic corrosion process of MZC MG in pure water is very important for understanding the degradation of MZC in different solutions, which is actually the transition of Mg, Zn and Ca atoms losing their electronics and changing into ions. The detailed transition process is shown schematically in Figure 5.

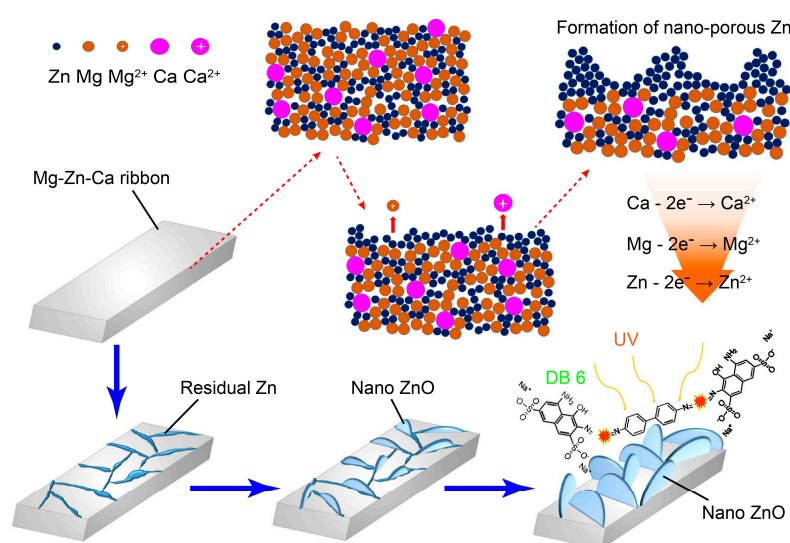


**Figure 5.** A schematic picture showing the mechanism in degrading azo dyes driven by the formation of ZnO nano-plates on the surface of MZC MG ribbon, the red sparkles refer to the breaking of azo bonds.

As is known, the chemical activity of metal elements is different, which has been regarded as the theoretical basis of dealloying [21]. In Mg-based and Ca-based MG, Mg and Ca are dissolved first, and other inactive elements, such as Cu, Y and Ag, are remained and formed into nanoporous materials [22]. Likewise, the order of the chemically active properties of the metal elements Mg, Zn and Ca is  $\text{Ca} > \text{Mg} > \text{Zn}$ . Ca and Mg are more likely to lose electrons than Zn and become ions, dissolving in aqueous solution to be degraded. Although all these Mg, Zn and Ca elements are typical degradable metals [23], their corrosion/degradation is not synchronized. As the other elements are dissolving at the initial stage, Zn stays as a relatively inactive element in the MZC alloy, and should remain, resulting in the formation of a thin nanoporous Zn layer. It can be verified by the XRD results for the MZC ribbons after immersion as shown in Figure 2. In our opinion, the remaining nanoporous Zn can easily transform to Zn-rich oxides or hydroxides, due to the effect of high specific surface area. We note that the network in Figure 2 shows a similar morphology to the flower-like  $\text{Zn}_5(\text{OH})_8\text{Cl}_2 \cdot \text{H}_2\text{O}$  or the ZnO nano-plate in the literature [24,25]. Therefore, it can be speculated that the nano-plate networks in Figure 2 are composed by ZnO or its derivatives. It is well known that ZnO has good photocatalytic effects and can degrade azo dyes under ultraviolet light (UV) [26,27]. In our opinion, the formation of ZnO on the surface of MZC ribbon could play an important role for degrading azo dyes.

The corrosion process of MZC in ASW is basically consistent with that in DW, except that the process is accelerated, which can be verified by the evolution of the corroded morphology in Figure 1.

In addition, the increment of pH value generally relates to the degradation of Mg, which increases the concentration of OH<sup>-</sup> ion in the solution [28]. In ASW, the metal elements in MZC MG are more likely to lose electrons into ions in comparison with those in DW, leading to the faster formation of ZnO-like nano-plates, which could be responsible for the rapid degradation of azo dyes.

Although ultrafine MZC powder has good degradation performance, further application might be limited due to oxidation in preparation and storage. The use of ribbons will reduce the cost of production, storage and transportation for oxidation protection. In particular, when the azo dye pollution happens in a sea environment, or the sewage is mixed with a certain proportion of seawater, the degradation efficiency will be greatly improved, which also shows that MZC MG ribbon is very suitable for use in coastal areas. In addition, the high efficiency of MZC MG in degrading azo dyes strongly depends on the state of the used materials. It has been reported that only the powders prepared by high-energy ball milling or atomization have high efficiency, and other forms of materials (in bulk, ribbon, line and so on) are rarely reported. We know that high-energy ball milling and spray atomizing both have high production costs, which might not conducive to wide commercial application. In this work, it is found that the melt-spun MZC MG ribbons also have high degradation efficiency when combined with NaCl. It is worth noting that the production cost of melt-spun ribbons is relatively low, enhancing the competitiveness of MZC MG in seawater treatment.

## 5. Conclusions

In the present work, the comparative corrosion behavior of Mg-Zn-Ca MG in DW and in ASW is studied. It is found that the basic corrosion process of Mg<sub>66</sub>Zn<sub>30</sub>Ca<sub>4</sub> MG in DW is similar to that in ASW, except that the detailed process of the latter is obviously accelerated. As-spun Mg<sub>66</sub>Zn<sub>30</sub>Ca<sub>4</sub> metallic glass shows a greater ability to degrade azo dyes in ASW solution, with a degradation efficiency over 100 times greater than that in DW solution. It is suggested that Mg-Zn-Ca MG are potential and promising sewage treatment agents in seawater. The rapid degradation of azo dyes can be attributed to the initially formed layer with Zn-enrich on the surface of MG, and thereafter the fast growth of ZnO nano-plates, inducing good photocatalytic effects combined with strong adsorption of azo dye molecules.

**Acknowledgments:** This work was supported by Hebei Education Department of China (Grant No. QN2014032), Hebei Provincial Department of Human Resources and Social Security of China (Grant No. B2015003012) and Natural Science Foundation of Hebei Province in China (Grant No. E2016202332 and E2016202406).

**Author Contributions:** Peng Chen and Xin Wang conceived and designed the experiments; Peng Chen, Ximei Hu, Yumin Qi and Zongjia Li performed the experiments; Xin Wang, Lichen Zhao, and Chunxiang Cui analyzed the data; Shuiqing Liu contributed materials tools; Peng Chen, Xin Wang and Chunxiang Cui wrote the paper.

**Conflicts of Interest:** The authors declare no conflict of interest.

## References

1. Wang, J.Q.; Liu, Y.H.; Chen, M.W.; Louzguine-Luzgin, D.V.; Inoue, A.; Perepezko, J.H. Excellent capability in degrading azo dyes by MgZn-based metallic glass powders. *Sci. Rep.* **2012**, *2*, 418. [[CrossRef](#)] [[PubMed](#)]
2. Zhao, Y.F.; Si, J.J.; Song, J.G.; Yang, Q.; Hui, X.D. Synthesis of Mg-Zn-Ca metallic glasses by gas-atomization and their excellent capability in degrading azo dyes. *Mater. Sci. Eng. B* **2014**, *181*, 46–55. [[CrossRef](#)]
3. Ramya, M.; Karthika, M.; Selvakumar, R.; Raj, B.; Ravi, K.R. A facile and efficient single step ball milling process for synthesis of partially amorphous Mg-Zn-Ca alloy powders for dye degradation. *J. Alloys Compd.* **2017**, *696*, 185–192. [[CrossRef](#)]
4. Ghidelli, M.; Gravier, S.; Blandin, J.J.; Pardoën, T.; Raskin, J.P.; Mompiau, F. Compositional-induced structural change in Zr<sub>x</sub>Ni<sub>100-x</sub> thin film metallic glasses. *J. Alloys Compd.* **2014**, *615*, S348–S351. [[CrossRef](#)]
5. Tang, Y.; Shao, Y.; Chen, N.; Yao, K.F. Rapid decomposition of Direct Blue 6 in neutral solution by Fe-B amorphous alloys. *RSC Adv.* **2015**, *5*, 6215–6221. [[CrossRef](#)]
6. Tang, Y.; Shao, Y.; Chen, N.; Liu, X.; Chen, S.Q.; Yao, K.F. Insight into the high reactivity of commercial Fe-Si-B amorphous zero-valent iron in degrading azo dye solutions. *RSC Adv.* **2015**, *43*, 34032–34039. [[CrossRef](#)]

7. Chen, S.Q.; Yang, G.N.; Luo, S.T.; Yin, S.J.; Jia, J.L.; Li, Z.; Gao, S.G.; Shao, Y.; Yao, K.F. Unexpected high performance of Fe-based nanocrystallized ribbons for azo dye decomposition. *J. Mater. Chem. A* **2017**, *27*, 14230–14240. [[CrossRef](#)]
8. Liu, S.; Cui, C.; Wang, X.; Li, N.; Shi, J.; Cui, S.; Chen, P. Effect of cooling rate on microstructure and grain refining behavior of in situ CeB<sub>6</sub>/Al composite inoculant in aluminum. *Metals* **2017**, *7*, 204.
9. Liu, S.; Wang, X.; Cui, C.; Zhao, L.; Li, N.; Zhang, Z.; Ding, J.; Sha, D. Enhanced grain refinement of in situ CeB<sub>6</sub>/Al composite inoculant on pure aluminum by microstructure control. *J. Alloys Compd.* **2017**, *701*, 926–934. [[CrossRef](#)]
10. Ghidelli, M.; Idrissi, H.; Gravier, S.; Blandin, J.-J.; Raskin, J.-P.; Schryvers, D.; Pardoën, T. Homogeneous flow and size dependent mechanical behavior in highly ductile Zr<sub>65</sub>Ni<sub>35</sub> metallic glass films. *Acta Mater.* **2017**, *131*, 246–259. [[CrossRef](#)]
11. Zhang, C.; Zhu, Z.; Zhang, H. Effects of the addition of Co, Ni or Cr on the decolorization properties of Fe-Si-B amorphous alloys. *J. Phys. Chem. Solids* **2017**, *110*, 152–160. [[CrossRef](#)]
12. Zhang, C.; Sun, Q. Annealing-induced different decolorization performances of Fe-Mo-Si-B amorphous alloys. *J. Non-Cryst. Solids* **2017**, *470*, 93–98. [[CrossRef](#)]
13. Xie, S.H.; Huang, P.; Kruzic, J.J.; Zeng, X.R.; Qian, H.X. A highly efficient degradation mechanism of methyl orange using Fe-based metallic glass powders. *Sci. Rep.* **2016**, *6*, 21947. [[CrossRef](#)] [[PubMed](#)]
14. Chen, S.; Chen, N.; Cheng, M.; Luo, S.; Shao, Y.; Yao, K. Multi-phase nanocrystallization induced fast degradation of methyl orange by annealing Fe-based amorphous ribbons. *Intermetallics* **2017**, *90*, 30–35. [[CrossRef](#)]
15. Zhao, Y.Y.; Ma, E.; Xu, J. Reliability of compressive fracture strength of Mg-Zn-Ca bulk metallic glasses: Flaw sensitivity and Weibull statistics. *Scr. Mater.* **2008**, *58*, 496–499. [[CrossRef](#)]
16. Liu, S.; Wang, X.; Cui, C.; Zhao, L.; Liu, S.; Chen, C. Fabrication, microstructure and refining mechanism of in situ CeB<sub>6</sub>/Al inoculant in aluminum. *Mater. Des.* **2015**, *65*, 432–437. [[CrossRef](#)]
17. Gu, X.; Shiflet, G.J.; Guo, F.Q.; Poon, S.J. Mg-Ca-Zn bulk metallic glasses with high strength and significant ductility. *J. Mater. Res.* **2011**, *20*, 1935–1938. [[CrossRef](#)]
18. Li, H.; Pang, S.; Liu, Y.; Sun, L.; Liaw, P.K.; Zhang, T. Biodegradable Mg-Zn-Ca-Sr bulk metallic glasses with enhanced corrosion performance for biomedical applications. *Mater. Des.* **2015**, *67*, 9–19. [[CrossRef](#)]
19. Greer, J.R.; De Hosson, J.T.M. Plasticity in small-sized metallic systems: Intrinsic versus extrinsic size effect. *Prog. Mater. Sci.* **2011**, *56*, 654–724. [[CrossRef](#)]
20. Ghidelli, M.; Sebastiani, M.; Johanns, K.E.; Pharr, G.M. Effects of indenter angle on micro-scale fracture toughness measurement by pillar splitting. *J. Am. Ceram. Soc.* **2017**, *100*, 5731–5738. [[CrossRef](#)]
21. Liu, X.; Chen, N.; Gu, J.L.; Du, J.; Yao, K.F. Novel Cu-Ag bimetallic porous nanomembrane prepared from a multi-component metallic glass. *RSC Adv.* **2015**, *62*, 50565–50571. [[CrossRef](#)]
22. Li, R.; Wu, N.; Liu, J.; Jin, Y.; Chen, X.-B.; Zhang, T. Formation and evolution of nanoporous bimetallic Ag-Cu alloy by electrochemically dealloying Mg-(Ag-Cu)-Y metallic glass. *Corros. Sci.* **2017**, *119*, 23–32. [[CrossRef](#)]
23. Zheng, Y.F.; Gu, X.N.; Witte, F. Biodegradable metals. *Mater. Sci. Eng. R* **2014**, *77*, 1–34. [[CrossRef](#)]
24. Mahmoudian, M.R.; Basirun, W.J.; Alias, Y.; Ebadi, M. Facile fabrication of Zn/Zn-5(OH)(8)Cl-2-H<sub>2</sub>O flower-like nanostructure on the surface of Zn coated with poly (N-methyl pyrrole). *Appl. Surf. Sci.* **2011**, *257*, 10539–10544. [[CrossRef](#)]
25. Su, P.P.; Zhao, J.; Rong, F.; Li, C.; Yang, Q.H. Fabrication of ZnO with tunable morphology through a facile treatment of Zn-based coordination polymers. *Sci. China Chem.* **2015**, *58*, 411–416. [[CrossRef](#)]
26. Daneshvar, N.; Salari, D.; Khataee, A.R. Photocatalytic degradation of azo dye acid red 14 in water on ZnO as an alternative catalyst to TiO<sub>2</sub>. *J. Photochem. Photobiol. A* **2004**, *162*, 317–322. [[CrossRef](#)]
27. Kansal, S.K.; Singh, M.; Sud, D. Studies on photodegradation of two commercial dyes in aqueous phase using different photocatalysts. *J. Hazard. Mater.* **2007**, *141*, 581–590. [[CrossRef](#)] [[PubMed](#)]
28. Zhao, L.C.; Cui, C.X.; Wang, X.; Liu, S.J.; Bu, S.J.; Wang, Q.Z.; Qi, Y.M. Corrosion resistance and calcium-phosphorus precipitation of micro-arc oxidized magnesium for biomedical applications. *Appl. Surf. Sci.* **2015**, *330*, 431–438. [[CrossRef](#)]

